Spatial Domain Filtering of Specific Frequencies: Curvature isolation of potential field signals

Madeline Lee, Hernan Ugalde, and Bill Morris, MAGGIC, School of Geography & Earth Sciences, McMaster University, Hamilton, Ontario, Canada*

Summary

Over the past few years there has been a dramatic increase in the volume of magnetic data becoming available, covering wider areas for which there is often limited priori geological information available. Coupled with a demand for faster data interpretation there has been an increased interest in the development of semi-automated data processing routines, which are designed to aid in delineating source body locations, geometries, and depths. These semi-automated methods may be applied in either a spatial or frequency domain, but there are assumptions that prevent the deduction of a geologically sound model. These assumptions include limited geological constraints and the infinite magnetic source. Through the application of a spatial domain filter that uses the curvature of a potential field signal, these assumptions may be avoided. By varying the grid cell size, thus the solution window, isolation of specific frequencies may be achieved which can then be used as a regional-residual separation scheme.

Introduction

With an ever increasing demand for quicker processing routines on larger potential field datasets, more efficient semi-automated processing routines are being developed. These routines are designed to aid in the delineation of source body locations, geometries, and depths. Most of these routines (e.g. Euler Deconvolution, Tilt-Angle) are based on computations that involve gradients of the magnetic or gravity field. A basic assumption of all these methods is that the data within an individual solution window defines a single isolated magnetic anomaly. These conditions are rarely met.

The Total Magnetic Intensity (TMI) signal at any single point represents the magnitude of the vector summation of all sources in proximity of the observation points. The ridges and troughs (anomalies) which characterize all TMI maps are a record of the interference from the various sources. Applying a semi-automated processing scheme to this type of mixed source data will produce many solutions that are not geologically meaningful. Utilisation of this information then necessitates some type of solution filter. Assuming a simple dual-layer structure one could attempt a source segregation through a regional-residual separation. Typically most regional-residual methods involve some aspect of FFT data processing. While the FFT approach has permitted rapid analysis of large data sets it is well-known that the methodology can produce geologically invalid outputs when some of the primary assumptions are violated.

Methodology

A magnetic signal can be described in respect to its curvature and can be defined as the rate of change in the direction of a curve in 2D. Roberts (2007) defines curvature as

$$\kappa = \frac{\partial \omega}{\partial S} = \frac{2\pi}{2\pi r} = \frac{1}{r} \qquad (1)$$

where $\partial \omega$ and ∂S are rates of change of angle and arc respectively. Based on the above equation, if the radius is large or the angle subtended by the arc is considerably small then the circle will have a small curvature (e.g. where $r = \infty$ will produce a straight line). If the radius is small (large angle versus arc rate of change, e.g. a small circle) then a large curvature is achieved.

A number of common semi-automated data processing schemes use some aspects of the curvature of a signal in order to delineate source geometries and depth (Thurston and Smith, 1997; Smith *et al*., 1998; Phillips, 2007). Mickus *et al.* (1991) presented a data processing technique using the minimum curvature gridding method in order to complete regional - residual separation on gravity data. Their proposed minimum curvature technique involved gridding the original dataset at an appropriate grid cell size and then desampled at a coarser grid cell size that was based on a feature of interest's size and data spacing. This coarsely gridded interpolation acted as a regional dataset and was subsequently subtracted from the original in order to delineate gravity anomalies (residual). This method was proposed as an alternative to the typical polynomial surface trend or FFT technique. Through the application of the minimum curvature technique and a polynomial trend surface to a field example, it was shown that that minimum curvature technique was capable of creating a more reliable residual field than the trend surface method. Mickus *et al.* (1991) discussed that there were still limitations to using minimum curvature and the method was best suited for shallow features at or near surface which had available geologic or geophysical data. The idea of using a varying grid cell size was further developed by Morris (2002), who discussed that it was possible to accentuate circular anomalies by using two grid cell sizes to create a range of the anticipated dimension of a source feature. Morris (2002) successfully isolated pipe-like features through the application of grid cell size variation.

The minimum curvature methods proposed by Mickus *et al.* (2007) and Morris (2002) can be further developed in respect to curvature. Wavelength of a signal is inextricably linked to curvature, as a high-frequency signal will be represented by a large curvature while a low-frequency will be represented by a small curvature. To achieve isolation of a specific frequency, curvature identification may be implemented as an alternative to FFT. This curvature identification scheme would act instead as a spatial domain filter and could be accomplished through the variation of grid cell size. The grid cell size of the original data will have a direct effect on the resultant curvature of the magnetic signal and by varying the grid cell size, one can isolate what portion of a curve is being interpreted; for example a coarse grid cell size will represent low-frequency sources (deep) and a fine grid cell size will be associated with high frequency sources (shallow).

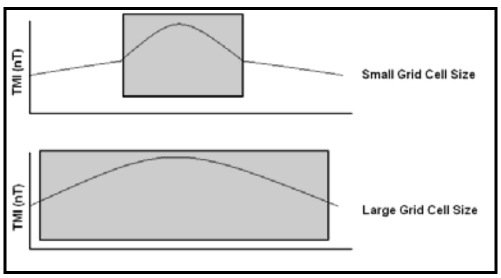

Figure 1: The scale of interpretation needs to be taken into consideration. When a small grid cell size is chosen, higher frequency anomalies will be resolved, while a coarser grid cell size will smooth high frequency noise, and only low frequency signals are resolved.

If we consider the total magnetic signal produced by a series of near-surface vertical-sided anomalous source bodies, the geometry of the resulting magnetic anomaly is dominated by the depth to the top of the sources and minimally from the bottom of them. As discussed by Spector and Grant (1970) the magnetic signal generated by a parallel-piped, vertical source is dominated by the depth to top of the source and minimally by its depth to bottom. This is true for most cases and as such the depth to bottom is typically not taken into consideration. However, it is in isolated instances that the depth to bottom does have a significant impact on the resultant anomaly, such as with very shallow, thin bodies. Again the observed field gradients represent a composite of sources. Theoretically one should be able to separate the magnetic anomaly associated with the base of the source body from that associated with the top of the source body by applying a regional - residual approach that separates the influence of top and bottom on the basis of their differing wavelength. One way in which signal interference has been mitigated is through regional-residual separation. In the case of regional-residual separation, the high-frequency noise and low-frequency noise are separated during the initial processing steps, so that all interpretations may be conducted on unbiased data. Over the years a number of different approaches to regional-residual signal separation have been suggested (Hearst *et al*., 2001; Li *et al.*, 1996). Most of these procedures invoke some aspect of FFT data processing. While the FFT approach has permitted rapid analysis of large data sets it is well-known that the methodology can produce geologically invalid outputs when some of the primary assumptions of are violated. Once again, by implementing a spatial-domain filter, these primary assumptions would be avoided.

Results

In order to investigate interference effects due to shallow, thin bodies, two synthetic models were generated: one at close proximities to the sensor with a shallow depth to bottom and one with an infinite depth to bottom. The synthetic models were comprised of three rectangular, vertical-sided prisms, 3km in length occurring in an ambient magnetic field of 60 000nT with an inclination and declination of 90˚ and 0˚ respectively. A flight line spacing of 100m and a sampling rate of 10m was used. Each prism had a magnetic susceptibility of 0.01emu/cm^3 and a distance of 10m between the top of body and sensor. The following were the resultant TMI signals generated by the two models.

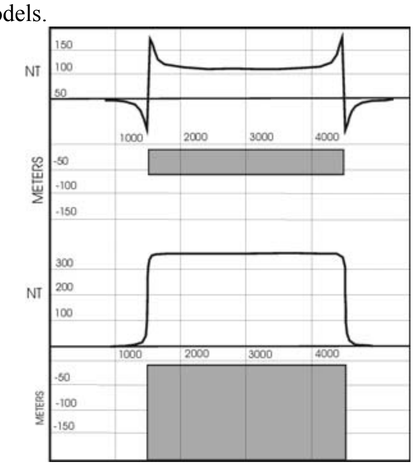

Figure 2. Cross-sections of the same rectangular prism, but with a depth to bottom of 60m (top) and the other with a depth to bottom of 20km, to approximate infinite (bottom). This plot displays the interference between the top and bottom of the source body on the resultant TMI signal.

Thus it is apparent that the depth to bottom does have an influence over the resultant TMI anomaly in specific instances. In order to remove the effect of bottom signal, the original dataset was gridded equivalent to the line spacing (100m) and then a coarser grid cell size of 1000m was gridded in order to isolate amplify only the low frequency signal (regional). Subsequently the regional grid was subtracted from the original in order to isolate the high-frequency signal (residual).

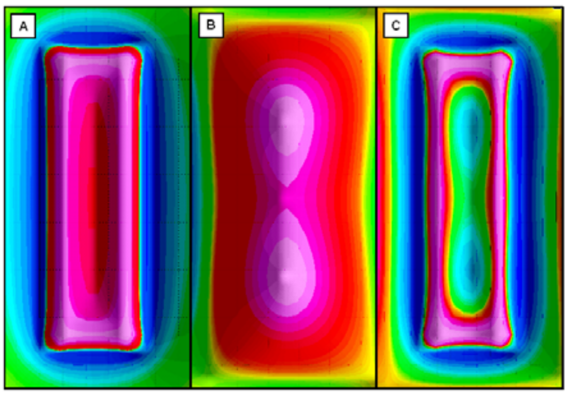

Figure3: Plots of Total Magnetic Intensity. A) Original TMI dataset gridded at 100m B) Regional TMI dataset gridded at 1km C) Residual TMI dataset produced by the subtraction of B) from A).

The resultant residual TMI grid displays the signal contribution from depth to bottom. It is at this point that secondary processing and interpretation routines may be applied to the unbiased data.

Application: Iroquois Falls, Ontario

The data used in this field example has been acquired from high-resolution MIDAS horizontal magnetic gradient survey over Porcupine Destor-Pipestone Faults area near Iroquois Falls and Matheson, Ontario. The helicopter survey was flown in 2003 and 2004 by Fugro Airborne Surveys Corp. with a line spacing of 75m, with a terrain clearance of 15m above the tallest surface feature. This region is predominantly Archean greenstone and as such contributes high frequency signals, similar to those seen with local kimberlites.

The simple grid subtraction routine was implemented. Initially, the dataset was gridded at ¼ the line space (20m) and then subsequently gridded at a coarser grid cell size of 640m. This coarse grid represented only the long wavelength features in the study area (regional). When the regional was subtracted from the original dataset, a residual dataset was produced, delineating the high-frequency features in the region, including all faults and dykes.

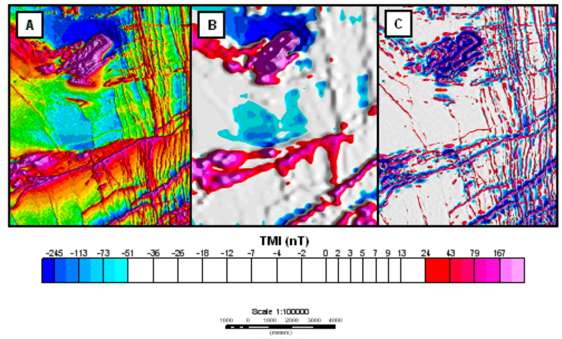

Figure 4: Plots of total magnetic field from Iroquois Falls region. A) Original TMI dataset gridded at 20m. B) Regional TMI dataset gridded at 640m. C) Residual TMI dataset produced by the subtraction of B) from A).

Subsequently, the depth estimating technique of tilt-angle was applied to the above results. Tilt-angle was first introduced by Miller and Singh (1994) and has since been defined as:

$$\theta = \tan^{-1}\left(\frac{\partial M/\partial z}{\partial M/\partial h}\right) \qquad (2)$$

where $$\frac{\partial M}{\partial h} = \sqrt{\left(\frac{\partial M}{\partial x}\right)^2 + \left(\frac{\partial M}{\partial y}\right)^2} \qquad (3)$$

and $$\frac{\partial M}{\partial x}, \frac{\partial M}{\partial y}, \frac{\partial M}{\partial z} \qquad (4)$$

which are first-order derivatives of the magnetic field (M) in the directions of x, y, and z. Since tilt-angle is a trigonometric function (arctan) all resultant values are between -90˚ and +90˚. Miller and Singh (1994) showed that tilt-angle was capable of edge detection and delineation of source body orientation. Salem *et al.* (2007a., 2007b.) introduced the concept that tilt-angle could be used as a simple method to delineate the depth to top of source. Salem *et al.* (2007a., 2007b.) extended the tilt-angle expression in order to derive a relationship between the horizontal location of a contact (*h*) and the depth to top of source (z_T):

$$\theta = \tan^{-1}\left(\frac{h}{z_T}\right) \qquad (5)$$

According to Salem et al. (2007a., 2007b.) when the results of tilt-angle are calculated and contoured, it is shown that the physical distance between -45˚ and +45˚ is equivalent to twice the depth to top ($2z_T$). Furthermore, that the 0˚ contour is equivalent to the source body contact (h=0). This depth estimation routine could be further enhanced through the application of the grid cell separation scheme as a pre-processing step.

Salem et al. (2007a., 2007b.) discussed that the tilt-angle process was to be applied in a perfectly vertical ambient magnetic field, as such RTP was applied to the Iroquois Falls dataset prior further processing. Tilt-angle was applied to the original TMI grid and the computed regional and residual grids. As was expected, the regional grid produced tilt-angle solutions at greater depths, while the residual grid produced shallow solutions. When focusing on the geological structure located in the north section of the study area, the tilt-angle indicated the feature began at a depth of 50m and extended to a minimum of 255m below the sensor. When comparing the solution depths between the original TMI and residual TMI, there was a discrepancy of 25m, which can be accounted for in the deconvolution of signals during the regional-residual separation scheme.

By creating an upper (residual) and lower (regional) extent of interpretation, we are in turn creating a "depth slice", a narrowed perspective of a specific region below surface. By varying the upper and lower extents, we can vary what subsurface slice is being observed. In order to view the effects of changing the lower extent, a regional trend of 320m grid cell size was computed and tilt-angle recomputed. The results over the northern geologic feature can be seen in figure 5. The thinner depth slice (20m-320m) produced features at shallower depths while the thicker depth slice (20m-640m) delineated the feature at a greater depth (an average depth solution difference between the two depth slices was 10m).

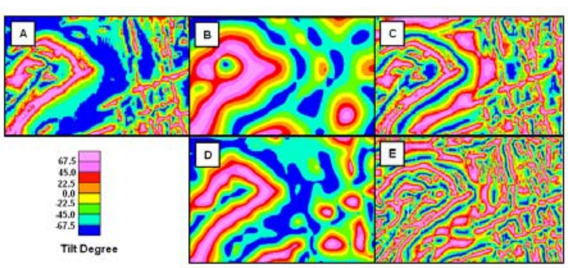

Figure 5: Tilt-Angle applied to varying grid cell sizes and depth slices of the Iroquois Falls dataset. A) Original TMI dataset gridded at 20m. B) Regional TMI dataset gridded at 640m. C) Residual TMI dataset produced by the subtraction of A) from B). D) Regional TMI dataset gridded at 320m. E) Residual TMI dataset produced by the subtraction of D) from A).

Subsequently, two depth slices were computed in order to compare the solutions resolved at varying depth slice location below surface. Both slices were equal to 4n, where n is the grid cell size of the original TMI grid. The depth slices using a finer grid cell size (80m-320m), resolved the sources at shallower depths, while the depth slice utilizing coarser grid cells (160m-640m) resolved features at greater depths (figure 6). The deeper depth slice produced solution depths of 75m for the northern geologic structure, while the shallower depth slice produced a depth 60m, which makes sense since in the previous depth calculations the feature was to extend from 50m to a minimum of 255m below sensor.

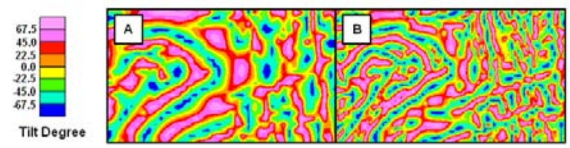

Figure 6: Tilt-Angle applied to varying depth slices of the Iroquois Falls dataset. A) Residual TMI dataset produced by the subtraction of 640m grid from 160m grid. B) Residual TMI dataset produced by the subtraction of 320m grid from the 80m grid.

Conclusions

Curvature interpretation of potential field datasets acts as a simple spatial domain filter; by doing so, many primary assumptions in the conventionally used FFT can be avoided. Furthermore, when curvature isolation is implemented in combination with grid cell size, the method allows for a quick regional – residual separation method. In order to efficiently isolate key frequencies, careful selection of the appropriate grid cell size must be completed. Curvature isolation methodology may be implemented as a pre-processing routine to semi-automated processing techniques, including Euler Deconvolution and Tilt-Angle. By varying the upper and lower depth boundaries, we are able to isolate source features at specific depths, and in combination with Tilt-Angle, the subsurface structure may be resolved in a series of slices.

EDITED REFERENCES

Note: This reference list is a copy-edited version of the reference list submitted by the author. Reference lists for the 2008 SEG Technical Program Expanded Abstracts have been copy edited so that references provided with the online metadata for each paper will achieve a high degree of linking to cited sources that appear on the Web.

REFERENCES

Hearst, R. B., and W. A. Morris, 2001, Case history: Regional gravity setting of the Sudbury Structure: Geophysics, **66**, 1680–1690.

Keating, P., and M. Pilkington, 2004, Euler deconvolution of the analytic signal and its application to magnetic interpretation: Geophysical Prospecting, **52**, 165–182.

Li, Y., and D. W. Oldenburg, 1996, 3D inversion of magnetic data: Geophysics, **61**, 394–408.

Miller, H. G., and V. Singh, 1994, Potential field tilt—A new concept for location of potential field sources: Applied Geophysics, **32**, 213–217.

Phillips, J. D., R. O. Hansen, and R. J. Blakely, 2007, The use of curvature in potential-field interpretation: Exploration Geophysics, **38**, 111–119.

Reid, A. B., J. M. Allsop, H. Granser, A. J. Millet, and I. W. Somerton, 1990, Magnetic interpretation in three dimensions using Euler deconvolution: Geophysics, **55**, 80–91.

Roberts, A., 2001, Curvature attributes and their application to 3D interpreted horizons: First Break, **19**, 85–100.

Thurston, J. B., and R. S. Smith, 1997, Automatic conversion of magnetic data to depth, dip, and susceptibility contrast using the SPI (TM) method: Geophysics, **62**, 807–813.

Salem, A., S. William, D. Fairhead, D. Ravat, and R. Smith, 2007a, Tilt-depth method: A simple depth estimation method using first-order magnetic derivatives: The Leading Edge, 1502–1505.

Salem, A., S. William, D. Fairhead, R. Smith, and D. Ravat, 2007b, Interpretation of magnetic data using tilt-angle derivatives: Geophysics, **73**, L1–L10.

Spector, A., and F. S. Grant, 1970, Statistical models for interpreting aeromagnetic data: Geophysics, **35**, 293–302.